Cellular Morphogenesis in the *Saccharomyces cerevisiae* Cell Cycle: Localization of the *CDC3* Gene Product and the Timing of Events at the Budding Site

Hyong Bai Kim, Brian K. Haarer, and John R. Pringle

Department of Biology and Program in Cellular and Molecular Biology, The University of Michigan, Ann Arbor, Michigan 48109

Abstract. Budding cells of the yeast *Saccharomyces cerevisiae* possess a ring of 10-nm-diameter filaments, of unknown biochemical nature, that lies just inside the plasma membrane in the neck connecting the mother cell to its bud. Electron microscopic observations suggest that these filaments assemble at the budding site coincident with bud emergence and disassemble shortly before cytokinesis (Byers, B. and L. Goetsch. 1976. *J. Cell Biol.* 69:717-721). Mutants defective in any of four genes (*CDC3*, *CDC10*, *CDC11*, or *CDC12*) lack these filaments and display a pleiotropic phenotype that involves abnormal bud growth and an inability to complete cytokinesis. We showed previously by immunofluorescence that the *CDC12* gene product is probably a constituent of the ring of 10-nm filaments (Haarer, B. and J. Pringle. 1987. *Mol. Cell. Biol.* 7:3678-3687). We now report the use of fusion proteins to generate polyclonal antibodies specific for the *CDC3* gene product. In immunofluorescence experiments, these antibodies decorated the neck regions of wild-type and mutant cells in patterns suggesting that the *CDC3* gene product is also a constituent of the ring of 10-nm filaments. We also used the *CDC3*-specific and *CDC12*-specific antibodies to investigate the timing of localization of these proteins to the budding site. The results suggest that the *CDC3* protein is organized into a ring at the budding site well before bud emergence and remains so organized for some time after cytokinesis. The *CDC12* product appears to behave similarly, but may arrive at the budding site closer to the time of bud emergence, and disappear from that site more quickly after cytokinesis, than does the *CDC3* product. Examination of mating cells and cells responding to purified mating pheromone revealed novel arrangements of the *CDC3* and *CDC12* products in the regions of cell wall reorganization. Both proteins were present in normal-looking ring structures at the bases of the first zygotic buds.

THE cell cycle of the yeast *Saccharomyces cerevisiae* involves a series of morphogenetic events including highly localized changes in the cell surface (7, 34, 40). As in other eukaryotes, elements of the cytoskeleton are believed to play key roles in these morphogenetic events. In addition to microtubules (2, 4, 18, 19, 21) and actin-containing structures (2, 21, 30), yeast cells contain another cytoskeletal element, of uncertain biochemical nature, that may be involved in morphogenesis. This is a highly ordered array of filaments, ~10 nm in diameter, that lies immediately subjacent to the cellular membrane in the region of the mother-bud neck (4, 5). By EM, these filaments seem to appear at the onset of bud emergence and to disappear just before cytokinesis. Temperature-sensitive mutants defective in any of four different genes (*CDC3*, *CDC10*, *CDC11*, and *CDC12*) lack these filaments and display a pleiotropic phenotype when shifted to restrictive temperature (Byers, B., and L. Goetsch. 1976. *J. Cell Biol.* 70:35a; 1, 2, 10, 13, 33; B. Byers and L. Goetsch, personal communication). The mutants are defective in cytokinesis, yet continue budding, DNA synthesis, and nuclear division, resulting in the formation of multibudded, multinucleate cells. In addition, the mutants fail to localize chitin properly to the bases of buds formed at restrictive temperature (1), and these buds are grossly elongated in comparison with normal buds (2, 13).

Recently, we localized the *CDC12* gene product to the vicinity of the 10-nm filaments using immunofluorescence with antibodies raised against fusion gene products (10). This observation together with the disappearance of the filaments in *cdc12* mutants suggests that the *CDC12* product is a constituent of the filaments. We now report the preparation of antibodies specific for the *CDC3* gene product and their use to localize this product in a pattern quite similar to that

Hyong Bai Kim's present address is Department of Biotechnology, Korea University, Chochiwon Chung Nam, 339-800 Korea. Brian K. Haarer's present address is Department of Anatomy and Cell Biology, The University of Michigan, Ann Arbor, Michigan 48109.

of the *CDC12* product. In addition, we have used the *CDC3*-specific and *CDC12*-specific antibodies to investigate the timing of filament assembly and disassembly relative to other landmark events at the beginning and end of the cell cycle. We have also used the antibodies to ask whether structures similar to the filament ring of budding cells appear during the morphogenetic response to mating pheromone (9, 26, 36, 41, 42), during zygote formation (28, 41, 43), and during formation of the first zygotic bud.

Materials and Methods

Reagents

Isopropyl β-D-thiogalactopyranoside, Ficoll (type 400), and alpha factor were obtained from Sigma Chemical Co. (St. Louis, MO). Rhodamine-conjugated goat anti-rat IgG (IgG fraction) was obtained from United States Biochemical Corporation (Cleveland, OH), and rat monoclonal anti-yeast-tubulin antibody (YOL1/34) was provided by J. Kilmartin (22). Other reagents were as described previously (10).

Genetic and Recombinant-DNA Manipulations

Standard procedures were used for recombinant-DNA manipulations (27), *E. coli* and yeast transformations (17, 27), and yeast genetic manipulations (37).

Plasmids, Strains, and Growth Conditions

Plasmid pUR290 (35) and *E. coli* strain BMH 71-18 (29) were provided by R. Schekman and were handled essentially as described previously (35). Plasmid pATH2 was provided by T. Koerner and A. Tzagoloff and was propagated in *E. coli* strain HB101 (27) essentially as described previously (10). Other plasmids are described in reference 25 or in Results.

The yeast strains used are listed in Table I. Except as noted, these were grown with rotary shaking in the rich, glucose-containing medium YM-P (24) at ~23°C. Strain TD4 was propagated in the appropriate selective minimal media (10) either without plasmid or after transformation with appropriate plasmids. Temperature-sensitive cell-division-cycle mutant strains were grown to ~10^7 cells/ml at ~23°C, then shifted to 36°C either without dilution or by diluting sixfold with fresh, prewarmed medium.

Alpha-Factor Arrest, Mating, and Synchronization

To arrest cell proliferation with alpha factor, strain CP1AB-1AA was grown to ~10^7 cells/ml, then diluted in fresh medium to a density of 2×10^6 cells/ml. Alpha factor was then added (from a 1-mg/ml stock in water) to a final concentration of 5 μg/ml and incubation was continued. For mating experiments, strains C276-4A and C276-4B were grown to ~10^7 cells/ml. Equal numbers of cells of opposite mating types were mixed and collected on 0.45-μm filters to yield 4×10^6 to 4×10^7 cells per 2.5-cm diameter filter. The filters were placed on YEPD plates and cells were collected after various periods of incubation by washing a filter with two 5-ml changes of phosphate buffer and adding formaldehyde to a final concentration of 3.7%. Alternatively, the haploid strains were grown to ~0.5×10^7 cells/ml, cultures were mixed so as to provide equal numbers of cells of each mating type, and incubation was continued with slow rotary shaking.

Two methods were used to obtain partially synchronized populations of budding cells. In the first, strain C276 cells were grown to early stationary phase and small cells were isolated using a Ficoll (mol wt 400,000) step-density gradient. 2 ml of culture were layered on a gradient of 4, 5, 6, and 7% Ficoll in sterile water (32 ml in a 50-ml centrifuge tube) and spun in a Sorvall GLC-2B tabletop centrifuge for 5 min at 800 rpm at ~23°C. Approximately 3 ml from the top of the gradient were removed and the cells in this fraction were harvested by spinning for 10 min at 1,500 rpm. These cells were predominantly unbudded and bud scar free (as judged by Calcofluor staining; 10, 40). The cells were washed with 10 ml of YM-P medium to remove the remaining Ficoll and were then resuspended and incubated in 10 ml of fresh medium. In the second method, cells exposed to alpha factor for 160 min as described above were harvested by centrifugation at ~23°C, then resuspended and incubated in an equal volume of fresh medium.

Preparation of Antigens and Antibodies

The *lacZ:CDC3* fusion protein was prepared from strain BMH 71-18 har-

Table I. Saccharomyces cerevisiae Strains Used in this Study

Strain	Relevant genotype	Source/reference
C276	*MATa/MATα* (Ts^+, prototrophic)	44
C276-4A	*MATa* (Ts^+, prototrophic)	44
C276-4B	*MATα* (Ts^+, prototrophic)	44
CP1AB-1AA	*MATa/MATa* (diploid)	31
TD4	*MATa ura3-52 his4-519 leu2-3,112 trp1-289*	G. Fink
LH104-HO1	*MATa/MATα cdc3-1/cdc3-1*	2
LH17012-HO1	*MATa/MATα cdc10-1/cdc10-1*	2
JPT194-HO1	*MATa/MATα cdc11-6/cdc11-6*	2
JPTA1493-HO1	*MATa/MATα cdc12-6/cdc12-6*	2
314D5	*MATa/MATα cdc4-1/cdc4-1*	12
473D3	*MATa/MATα cdc5-1/cdc5-1*	L. Hartwell (14)
JPT176-HO1	*MATa/MATα cdc5-2/cdc5-2*	This study*
428D1	*MATa/MATα cdc13-1/cdc13-1*	8
7041-HO1	*MATa/MATα cdc14-1/cdc14-1*	This study‡
JPT143-HO1	*MATa/MATα cdc14-14/cdc14-14*	This study*
17017	*MATa cdc15-1*	14
JPT161-HO1	*MATa/MATα cdc15-28/cdc15-28*	This study*
281D5	*MATa/MATα cdc16-1/cdc16-1*	L. Hartwell (14)
H178-1-1	*MATa cdc17-1*	L. Hartwell (14)
14028-HO1	*MATa/MATα cdc18-1/cdc18-1*	This study§

* Mutants JPT176, JPT143, and JPT161 were isolated from strain C276-4A, characterized, and backcrossed essentially as described previously (2) by A. E. M. Adams (1). Complementation and linkage analyses showed that these strains carried mutations in genes *CDC5*, *CDC14*, and *CDC15*, respectively (1; B. K. Haarer, unpublished results); allele numbers were assigned to avoid overlap with those assigned previously (14, 20). JPT176-HO1 is the product of mating *MATa* and *MATα* segregants from the third backcross. JPT143-HO1 is the product of mating JPT143 to a *MATα* segregant from the first backcross. JPT161-HO1 is the product of mating *MATa* and *MATα* segregants from the first backcross.

‡ Strain 7041 (14) was crossed to C276-4B; *MATa* and *MATα* segregants were then mated to produce 7041-HO1.

§ Strain 14028 (14) was mated to its *MATα* derivative H149-1-3 (obtained from L. Hartwell) to produce 14028-HO1.

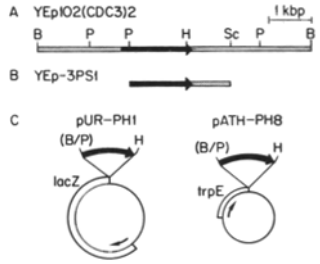

Figure 1. Structures of *CDC3*-containing plasmid inserts and of *lacZ:CDC3* and *trpE:CDC3* gene-fusion plasmids. (*A*) A 6.7-kbp Bam HI fragment was subcloned from plasmid YEp13(CDC3)1 (reference 25) into the pBR322-derived Bam HI site of the yeast-*E. coli* shuttle vector YEp102 to produce the *cdc3*-complementing plasmid YEp102(CDC3)2 (reference 25). (*B*) A 2.4-kbp Pvu II–Sca I fragment was subcloned from YEp13(CDC3)1 into the pBR322-derived Pvu II site of YEp102 to produce the *cdc3*-complementing plasmid YEp-3PS1 (reference 25). (*C*) The 1.3-kbp Pvu II-Hind III fragment from YEp-3PS1 was inserted into the fusion vectors pUR290 and pATH2 to produce plasmids pUR-PH1 and pATH-PH8, respectively. In each case, the vector was linearized with Bam HI, treated with the Klenow fragment of DNA polymerase to produce blunt ends, digested with Hind III, and then ligated to the gel-purified Pvu II–Hind III fragment. Thick arrows represent the *CDC3* coding region as inferred from DNA sequence analysis (11), and stippled boxes represent adjacent yeast DNA. Open boxes represent the *lacZ* and *trpE* coding regions and thin lines represent other *E. coli* DNA. Thin arrows indicate the directions of transcription for the fusion genes. Restriction sites are indicated: (*B*), Bam HI; *H*, Hind III; *P*, Pvu II; *Sc*, Sca I; (*B/P*), Bam HI–Pvu II junction.

boring fusion plasmid pUR-PH1 (see Results). Cells were grown overnight in LB medium plus ampicillin (50 μg/ml) at 37°C, then diluted 1:10 in the same medium and grown 1 h at 37°C. Isopropyl β-D-thiogalactopyranoside (25 mg/ml in H_2O) was added to a final concentration of ~90 μg/ml, and cultures were grown for two more hours at 37°C. Cells were then harvested, resuspended in loading buffer (10), and placed in a boiling water bath for 1 to 2 min before loading samples on a polyacrylamide gel (10). The *trpE:CDC3* fusion protein was prepared from *E. coli* strain HB101 containing plasmid pATH-PH8 (see Results). Induction of the fusion protein and isolation of an insoluble protein fraction were essentially as described previously (10) for the *trpE:CDC12* fusion proteins. For immunization, both *CDC3* fusion proteins were purified from polyacrylamide gel slices and injected separately into rabbits as described previously (10).

CDC3-specific antibodies were affinity purified from crude anti-*trpE:CDC3* antiserum using the *lacZ:CDC3* fusion protein blotted to nitrocellulose as described previously (10, 23). In the same manner, *CDC3*-specific antibodies were purified from crude anti-*lacZ:CDC3* antiserum using nitrocellulose-bound *trpE:CDC3* fusion protein. *CDC12*-specific antibodies were prepared as described previously (10).

Indirect Immunofluorescence and Other Methods

Cells were ordinarily fixed by the addition of 37% formaldehyde directly to the culture medium (to a final concentration of 3.7%), then examined by phase-contrast microscopy (32) or washed and prepared for indirect immunofluorescence as described previously (2, 10, 21). Double-label experiments used FITC-conjugated goat anti-rabbit IgG to visualize rabbit anti-*CDC3* or anti-*CDC12* antibodies, plus rhodamine-conjugated goat anti-rat IgG to visualize rat antitubulin antibodies. Chitin rings were visualized by staining with Calcofluor as described previously (10, 40). Other methods were as described previously (10, 32).

Results

Construction of lacZ:CDC3 and trpE:CDC3 Gene Fusions

From the *CDC3*-containing plasmid YEp13(CDC3)1, a 2.4-kbp Pvu II–Sca I fragment was subcloned into the yeast-*E. coli* shuttle vector YEp102 to create plasmid YEp-3PS1 (ref 25; Fig. 1 *B*). Although this plasmid retains *cdc3*-complementing activity, sequence analysis suggests that it does not contain the entire *CDC3* coding region (11, 25; Fig. 1, *A* and *B*; and see below). To create a *lacZ:CDC3* fusion gene, the 1.3-kbp Pvu II Hind III fragment from YEp-3PS1 was inserted into plasmid pUR290 (35) to produce plasmid pUR-PH1 as shown in Fig. 1 *C*. Analysis of the *CDC3* sequence (11) indicated that this arrangement would result in an in-frame fusion of the *lacZ* and *CDC3* genes. Indeed, pUR-PH1 directed the synthesis of a ~160-kD fusion protein (Fig. 2 *A*, lanes *1–3*) when propagated under inducing conditions. A *trpE:CDC3* fusion gene was constructed by inserting the same Pvu II–Hind III fragment into plasmid pATH2 to produce plasmid pATH-PH8 as shown in Fig. 1 *C*. This plasmid

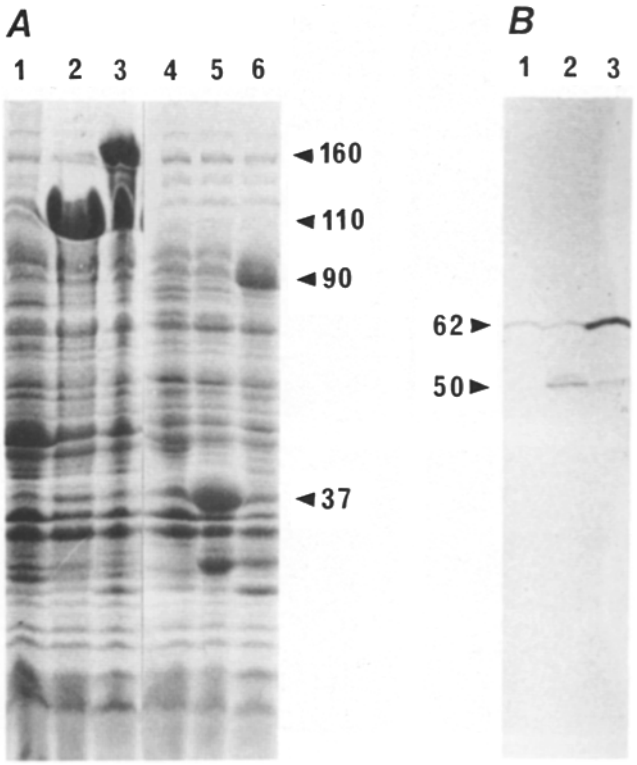

Figure 2. (*A*) Identification of *lacZ:CDC3* and *trpE:CDC3* fusion proteins by SDS-PAGE. (lanes *1–3*) Total proteins prepared from *E. coli* strain BMH 71-18 containing (Lane *1*) no plasmid; (lane *2*) plasmid pUR290; or (lane *3*) plasmid pUR-PH1. (Lanes *4–6*) Total proteins prepared from *E. coli* strain HB101 containing (lane *4*) no plasmid; (lane *5*) plasmid pATH2; or (lane *6*) plasmid pATH-PH8. In all cases, strains were propagated under inducing conditions as described in Materials and Methods. The approximate sizes of the truncated *lacZ* and *trpE* proteins encoded by the vectors and of the fusion proteins are given in kD. (*B*) Identification of the *CDC3* product in blots of yeast proteins using affinity-purified antibodies. (Lanes *1–3*) total cellular proteins were isolated from strain TD4 containing (lane *1*) plasmid YEp102 (ref. 25); (lane *2*) plasmid YEp-3PS1 (reference 25; Fig. 1 *B*); or (lane *3*) plasmid YEp102-(CDC3)2 (ref. 25; Fig. 1 *A*). Primary antibody used for all lanes was a 1:50 dilution of affinity-purified anti-*trpE:CDC3*. Secondary antibody used was a 1:100 dilution of HRP-conjugated goat anti-rabbit IgG. The position of the putative wild-type *CDC3* protein at ~62 kD is indicated, as is the truncated product (at ~50 kD) encoded by plasmid YEp-3PS1. The faint bands in lane *3* are presumed to be breakdown products of the overproduced 62-kD protein.

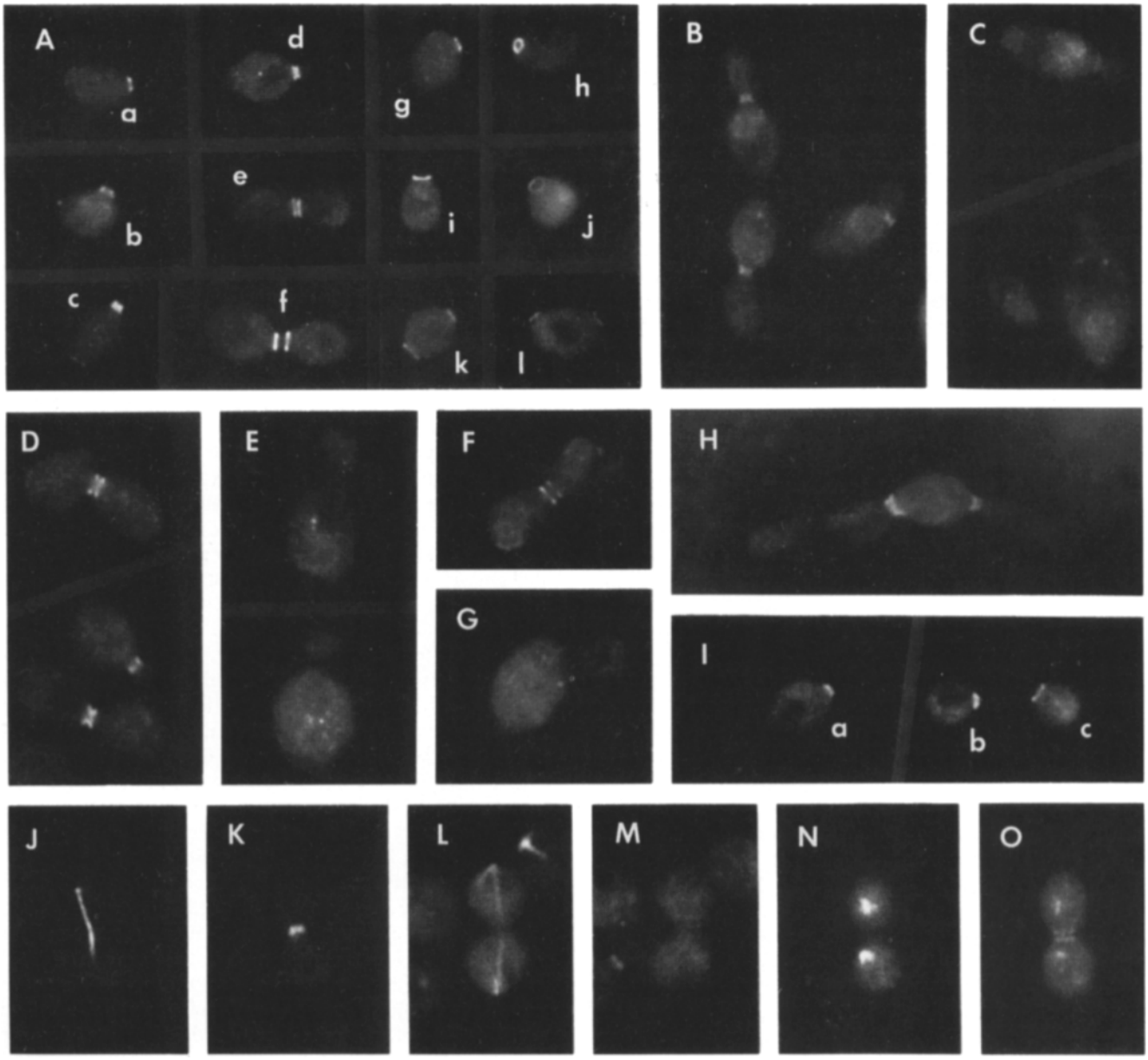

Figure 3. Immunofluorescence localization of the *CDC3* and *CDC12* gene products in wild-type and mutant cells. (*A* and *I*) C276 (wild-type) cells stained with anti-*trpE*:*CDC3* antibodies (*A*) or anti-*lacZ*:*CDC12* antibodies (*I*). Individual cells are labeled for reference in the text. (*B* and *C*) LH104-HO1 (*cdc3*) cells grown at 23°C (*B*) or at 36°C for 30 min (*C*) and stained with anti-*trpE*:*CDC3* antibodies. (*D* and *E*) LH17012-HO1 (*cdc10*) cells grown at ~23°C (*D*) or at 36°C for 30 min (*E*) and stained with anti-*trpE*:*CDC3* antibodies. (*F* and *G*) JPTA1493-HO1 (*cdc12*) cells grown at ~23°C (*F*) or at 36°C for 30 min (*G*) and stained with anti-*trpE*:*CDC3* antibodies. (*H*) 314D5 (*cdc4*) cells stained with anti-*trpE*:*CDC3* antibodies after growth at 36°C for 4 h. (*J–O*) C276 cells double stained with antitubulin antibodies (*J*, *L*, and *N*) and either anti-*trpE*:*CDC3* (*K* and *O*) or anti-*lacZ*:*CDC12* (*M*) antibodies. Affinity-purified rabbit anti-*trpE*:*CDC3* and anti-*lacZ*:*CDC12* antibodies were used at 1:3 dilution; FITC-conjugated goat anti-rabbit IgG secondary antibody was used at 1:40 dilution; rat antitubulin antibody was used at 1:100 dilution; and rhodamine-conjugated goat anti-rat IgG secondary antibody was used at 1:200 dilution. In the cells stained with antitubulin antibodies, some fluorescence from the rhodamine label is visible when viewing for FITC fluorescence (*K*, *M*, and *O*). Cells were photographed and printed at somewhat different sizes to show optimum detail; magnifications are ~1,300–2,000-fold.

directed the synthesis of a ~90-kD fusion protein (Fig. 2 *A*, lanes *4–6*) when propagated under inducing conditions.

Preparation of CDC3-specific Antibodies and Identification of the CDC3 Protein

The *lacZ*:*CDC3* and *trpE*:*CDC3* fusion proteins were used to elicit antibody production and the resulting antisera were tested by immunoblotting for their ability to recognize proteins from the appropriate *E. coli* strains. We obtained sera raised against each fusion protein that were able to recognize both fusion proteins in Western blots (data not shown; see similar experiments with antisera raised against *CDC12* fusion proteins in reference 10). Thus, each serum appeared to contain antibodies specific for *CDC3* determinants that are common to the two fusion proteins.

The *CDC3*-specific antibodies were affinity purified using nitrocellulose-bound fusion proteins and the purified antibodies were used to identify the authentic *CDC3* product in blots of yeast proteins. A ~62-kD protein was recognized in blots of total protein from *CDC3*$^+$ cells containing no plasmid (data not shown) or plasmid YEP102 (Fig. 2 *B*, lane *1*). A protein of the same mobility was present at higher levels in extracts of the same strain harboring a high-copy-number plasmid containing the entire *CDC3* coding region (Fig. 2 *B*, lane *3*), indicating that the ~62-kD protein is the authentic *CDC3* gene product. In addition, a plasmid containing a truncated *CDC3* coding region in the same strain directs the synthesis of a ~50-kD protein (Fig. 2 *B*, lane *2*; see Discussion).

Immunofluorescence Localization of the CDC3 Gene Product

Use of affinity-purified anti-*trpE:CDC3* (Fig. 3 *A*) or anti-*lacZ:CDC3* (data not shown) antibodies to stain wild-type yeast cells revealed a localization pattern very similar to that seen for the *CDC12* gene product (10). In cells with small buds, the *CDC3* gene product appeared in a single or double ring at the base of the bud (Fig. 3 *A*, cells *a–c*). In cells with medium or large buds, the *CDC3* gene product appeared as a pair of rings flanking the constriction of the mother-bud neck (Fig. 3 *A*, cells *d–f*). As noted previously (10), this appearance is that expected for an antigen present in a structure, such as the ring of 10-nm filaments, that follows the contour of the cell membrane through the neck region; thus, densest packing (in a two-dimensional projection), and therefore brightest fluorescence, would occur on the slopes of the mother and bud portions of the cell flanking the neck constriction. Finally, many unbudded cells also appeared to possess rings of *CDC3* antigen (Fig. 3 *A*, cells *g–l*), as considered further below.

Mutants defective in *CDC3*, *CDC10*, *CDC11*, or *CDC12* are unable to form or (at least for some alleles of *CDC10* and *CDC12*) maintain rings of 10-nm filaments at restrictive temperature (Byers, B., and L. Goetsch. 1976. *J. Cell Biol.* 70:35a; 1, 10). The pattern of *CDC3* product localization was examined in representative mutant strains. At permissive temperature, all four mutants displayed normal localization of the *CDC3* product (Fig. 3, *B*, *D*, and *F*), although the staining was somewhat diminished in *cdc3* (Fig. 3 *B*) and *cdc11* (strain JPT194-H01; data not shown) cells. After 30 min at restrictive temperature (sufficient to cause disappearance of 10-nm filaments [1; Byers, B., and L. Goetsch. 1976. *J. Cell Biol.* 70:35a] and delocalization of *CDC12* product [10] in the *cdc10* and *cdc12* cells), staining of *CDC3* product was not detectable in *cdc10* and *cdc12* cells (Fig. 3, *E* and *G*) and was greatly diminished or absent in *cdc3* cells (Fig. 3 *C*). *cdc11* cells showed only a minor reduction in staining intensity relative to the pattern observed at permissive temperature (data not shown). Moreover, a *cdc4* mutant strain (which also forms multiple, abnormally elongated buds at restrictive temperature, but has normal rings of 10-nm filaments) displayed apparently normal localization of *CDC3* product to the mother-bud necks even after several hours at restrictive temperature (Fig. 3 *H*). Thus, the results obtained with the mutant strains are also consistent with the hypothesis that the *CDC3* product is a constituent of the ring of 10-nm filaments.

Electron microscopic observations have suggested that the ring of 10-nm filaments appears coincident with bud emergence and disappears just before cytokinesis (4, 5). To begin exploring the behavior of the filament-associated polypeptides at the beginning and end of the budding cycle, we examined in detail the patterns of staining observed with *CDC3*-specific and *CDC12*-specific antibodies in exponentially growing wild-type cells. In a sample of strain C276, 62% of the cells were budded as judged by phase-contrast microscopy. Immunofluorescence revealed detectable rings of the *CDC3* and *CDC12* antigens in 96 and 80% of the total population, respectively. When we attempted to score the unbudded cells alone, we detected rings of *CDC3* and *CDC12* product in 93 and 40% of the cells, respectively. However, it should be noted that the latter counts are somewhat uncertain because small buds are difficult to see under the conditions used for immunofluorescence; thus, cells with small buds may be inadvertantly included in the counts, with the effect of inflating the apparent proportions of unbudded cells that possess rings of *CDC3* or *CDC12* antigen. Nonetheless, it seems clear that both antigens (and especially the *CDC3* product) must (*a*) be organized into a ring structure before bud emergence; (*b*) linger in a ring structure after cytokinesis; or (*c*) both. Support for possibility *c* is provided by the observation that the rings of antigen observed in unbudded cells appear to be of two types: first, a relatively narrow diameter, generally brightly staining structure (Fig. 3 *A*, cells *g*, *h*, and *k* [right-hand ring], and *l* [left-hand ring]; Fig. 3 *I*, cells *a* and *b*), such as would be expected if the structures observed at the bases of small buds (Fig. 3 *A*, cells *a–c*; Fig. 3, *D* and *E* of ref. 10) actually appeared in advance of bud emergence; and second, a relatively broad-diameter, generally less brightly staining structure (Fig. 3 *A*, cells *i*, *j*, and *k* [left-hand ring], and *l* [right-hand ring]; Fig. 3 *I*, cell *c*), such as would be expected if the structures of cells *e* and *f*, Fig. 3 *A*, were retained on mother and daughter cells after cytokinesis. The narrow and broad rings were present in ~35 and ~58%, respectively, of the apparently unbudded cells stained with *CDC3*-specific antibodies, and were each present in ~20% of the apparently unbudded cells stained with *CDC12*-specific antibodies. In addition, a small number of apparently unbudded cells (and even some cells with small buds) displayed coincidently both a narrow ring and a broad ring when stained with *CDC3*-specific antibodies (Fig. 3 *A*,

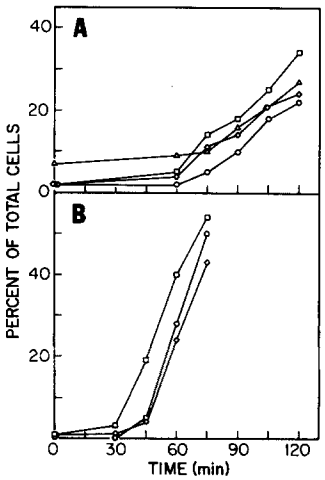

Figure 4. Timing of early events at the budding site in synchronized cultures. Partially synchronized budding was obtained (*A*) by isolating and culturing small unbudded cells of strain C276 or (*B*) by releasing cells of strain CP1AB-1AA from alpha factor arrest, as described in Materials and Methods. Samples taken at appropriate times were examined for the presence of buds (○), chitin rings (△), rings of *CDC3* protein (□), and rings of *CDC12* protein (◇).

cells *a*, *c*, *k*, and *l*), providing further support for possibility *c*, above. However, cells with two rings were not observed after staining with *CDC12*-specific antibodies.

Timing of Early Events at the Budding Site

To examine more closely the timing of the appearance of the *CDC3* and *CDC12* proteins at the budding site, small unbudded cells were isolated and cultured in fresh medium. The numbers of buds, chitin rings, and rings of *CDC3* or *CDC12* antigen were then compared during the partially synchronous round of budding that followed (Fig. 4 *A*). The initial cell population contained some cells with bud scars (i.e., chitin rings from previous budding cycles) but few or none with buds or with detectable rings of *CDC3* or *CDC12* antigen. Thus, at each time point, the total number of chitin rings is somewhat greater than the number of newly formed chitin rings, whereas the buds and antigen rings observed are presumably all newly formed. With this in mind, comparison of the curves in Fig. 4 *A* suggests that the *CDC3* and *CDC12* proteins localize to the budding site before bud emergence and apparently also before chitin ring formation. It should be noted, however, that immunofluorescence staining in the earlier samples (up to 75 min) seemed suboptimal, presumably because of difficulties in permeabilizing cells that were just emerging from stationary phase. Therefore, the counts of antigen rings in these early samples may have been distorted by a failure to detect some residual rings from earlier budding cycles, nascent rings from the new budding cycles, or both.

Because of this caveat, we also utilized a second method to synchronize budding. *MATa/MATa* diploid cells were treated with alpha factor to arrest the cells uniformly in the unbudded, G1 phase (33). After washing the cells and resuspending them in fresh medium, the numbers of buds and rings of *CDC3* or *CDC12* antigen were determined as a function of time. (The formation of new chitin rings could not be followed in this experiment because of the many bud scars present in the initial population.) Fig. 4 *B* shows that the rings of *CDC3* antigen appeared to form ~15 min before bud emergence, whereas the rings of *CDC12* antigen appeared to form approximately coincident with bud emergence. The apparent discrepancy between this and the other results on the timing of localization of the *CDC12* product is considered in the Discussion. It should be noted that the alpha factor experiments are subject to the caveat that alpha factor itself may perturb the normal distribution or assembly of the *CDC3* or *CDC12* protein (see also below).

Timing of Late Events at the Budding Site

We used three approaches to examine more closely the behavior of the *CDC3* and *CDC12* polypeptides at the end of the budding cycle. In the first approach, exponential-phase wild-type cells were examined by double-label immunofluorescence staining of tubulin and the *CDC3* or *CDC12* gene product. Cells were classified according to the appearance of their mitotic spindles, and the presence or absence of detectable rings of *CDC3* or *CDC12* antigen at the neck was noted. Both proteins appeared to remain localized to the neck region so long as an intact spindle was maintained (Fig. 3, *J* and *K*). As the spindle began to break down (late nuclear division), the *CDC12* protein seemed to disappear from the neck in most cells (Fig. 3, *L* and *M*). In contrast, the *CDC3* protein seemed to be retained at the neck until very late stages, and probably until after nuclear division and cytokinesis were complete (Fig. 3, *N* and *O*). The results are summarized in Table II.

In the second approach, we asked whether detectable rings of *CDC3* and *CDC12* proteins remained at the necks of various temperature-sensitive cell division cycle mutants that arrest late in the budding cycle at restrictive temperature (33). After 2–5 h at restrictive temperature, mutants arrested in medial nuclear division (*cdc13*, *cdc16*, and *cdc17*) or in late nuclear division (*cdc14* and *cdc15*) appeared consistently to maintain structures that contained both the *CDC3* and *CDC12* proteins (Fig. 5, *A–F*; and data not shown). Moreover, mutants arresting in very late nuclear division or between nuclear division and cytokinesis (*cdc5* and *cdc18*) also appeared to maintain the localization of the *CDC3* and *CDC12* proteins (Fig. 5, *G–N*), although the results with *cdc5* were somewhat heterogeneous. When strain 473D3 (*cdc5-1*) was grown at restrictive temperature for 2 h, by which time ~60% of the cells displayed large buds, detectable rings of *CDC3* and *CDC12* antigens were present in nearly all cells. Upon longer incubation at restrictive temperature, the population became very homogeneous (~95% large-budded cells) as judged by phase-contrast microscopy, but the proportions of cells displaying detectable rings of *CDC3* or *CDC12* antigen declined. By 5 h, only ~67 and ~15% of the cells displayed detectable rings of the *CDC3* and *CDC12* antigens, respectively. Consideration of the detailed time courses in these experiments (not shown) indicated that most or all cells must have been arrested with large buds for ≥1 h before the antigen rings disappeared. In addition, cells of strain JPT176-H01 (*cdc5-2*) retained detectable rings of both antigens on essentially all cells even after 5 h at restrictive temperature (Fig. 5, *I* and *M*; and data not shown), although staining with *CDC12*-specific antibodies was weak. Taken together, these observations suggest that disassembly of the *CDC3*-containing and *CDC12*-containing structures is not specifically programmed in cells that have reached the *cdc5* arrest point, and that the gradual disappearance of these structures in strain 473D3 (and of the *CDC12*-containing structures in strain JPT176-H01) reflects either a general cellular pathology or a slow leakage of the cells past the mutant block. The observation that tubulin immunofluorescence patterns also changed gradually in arrested 473D3 cells is consistent with either of the latter interpretations.

Table II. Localization of CDC3 and CDC12 Antigens in Wild-type Cells Late in the Budding Cycle

Spindle class*	Cells with detectable rings of	
	CDC3 antigen‡	*CDC12* antigen‡
	%	%
I	100	100
II	100	60
III	72	18

* Mitotic spindle classes were defined as follows: (*I*) cells having long spindles showing no evidence of disassembly (see Fig. 3 *J*); (*II*) cells having spindles in early stages of disassembly (see Fig. 3 *L*); and (*III*) cells showing no remaining spindle, but apparently still prior to cytokinesis (see Fig. 3 *N*).
‡ Percentages were based on counts of 50 cells for each sample.

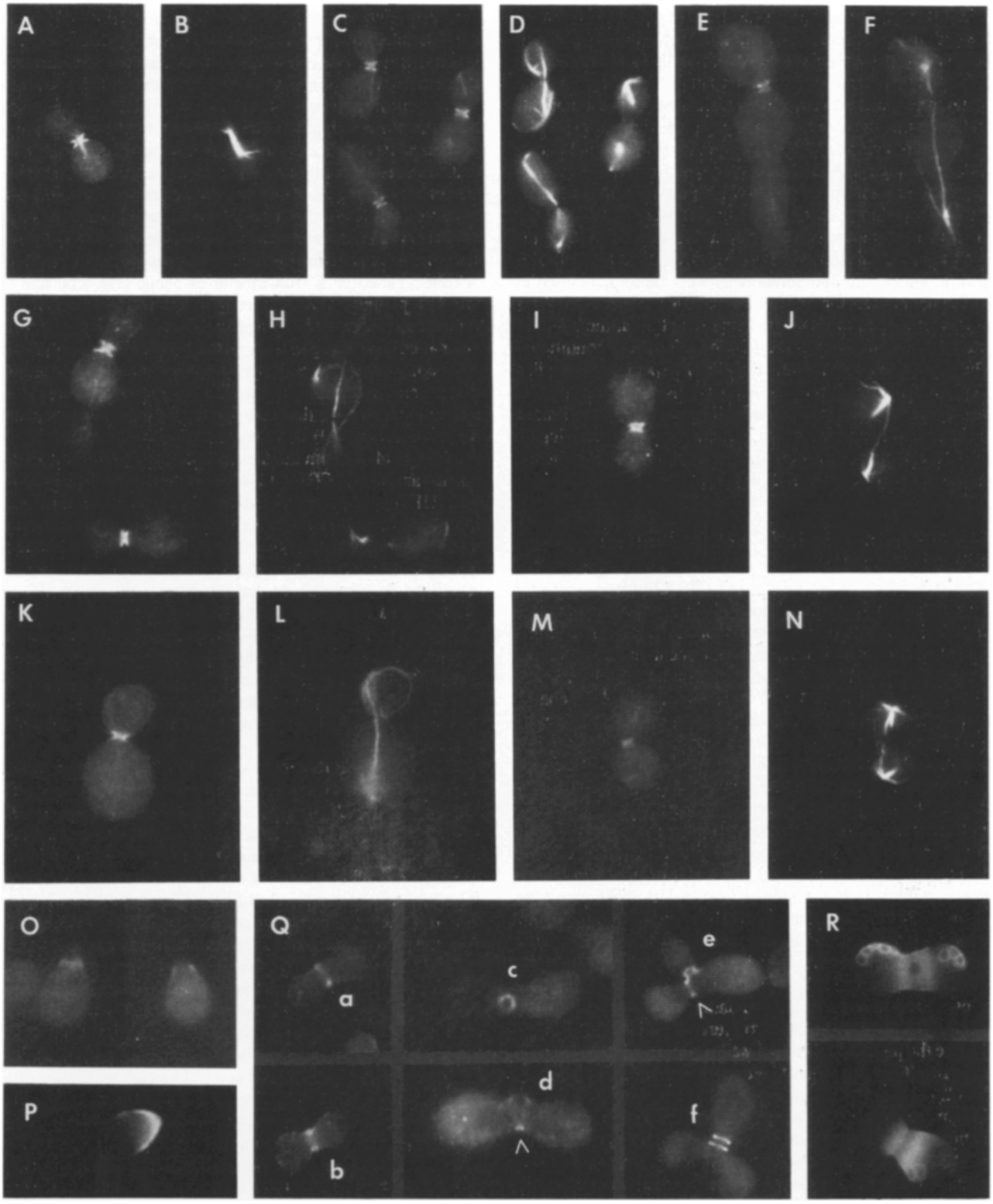

Figure 5. CDC3 and *CDC12* protein localization in nuclear division mutants, alpha factor arrested cells ("shmoos"), and zygotes. Primary and secondary antibody concentrations were as described in the legend to Fig. 3. (*A–N*) Mutant cells were double stained with antitubulin antibodies (*B, D, F, H, J, L,* and *N*) and with anti-*trpE:CDC3* antibodies (*A, C, G,* and *I*) or anti-*lacZ:CDC12* antibodies (*E, K,* and *M*). Some fluorescence from the rhodamine (tubulin) label is visible when viewing for FITC (*CDC3* or *CDC12*) fluorescence. (*A* and *B*) 281D5 (*cdc16*) cells after 7 h at 36°C. Similar results were obtained with strains 428D1 (*cdc13*) and H178-1-1 (*cdc17*). (*C* and *D*) JPT161-HO1 (*cdc15-28*) cells after 3 h at 36°C. Similar results were obtained with strain 17017 (*cdc15-1*). (*E* and *F*) JPT143-HO1 (*cdc14-14*) cells after 4 h at 36°C. Similar results were obtained with strain 7041-HO1 (*cdc14-1*). (*G, H, K,* and *L*) 14028-HO1 (*cdc18*) cells after 4 h at 36°C. (*I, J, M,* and *N*) JPT176-HO1 (*cdc5-2*) cells after 4 h (*I* and *J*) or 3 h (*M* and *N*) at 36°C. (*O* and *P*) Shmoo cells of strain CP1AB-1AA after treatment with alpha factor for 160 min, stained with anti-*trpE:CDC3* antibodies (*O*) or Calcofluor (*P*). (*Q* and *R*) Zygotes formed by mating strains C276-4A and C276-4B, stained with anti-*trpE:CDC3* antibodies (*Q*) or Calcofluor (*R*). Cells are labeled for reference in the text. Cells were photographed and printed at somewhat different sizes to show optimum detail; magnifications are ~1,300–2,000-fold.

The third approach to investigation of events at the end of the budding cycle involved treating an exponentially growing population of *MATa/MATa* cells with alpha factor to prevent new budding (and thus, presumably, formation of new budding-associated rings of the *CDC3* and *CDC12* antigens), and following the disappearance of preexisting antigen rings as the cells completed division and arrested as unbudded cells. Although the results were somewhat variable (apparently due at least in part to variations in the effectiveness of the immunofluorescence staining), it was clear that the proportion of unbudded cells displaying rings of *CDC3* antigen remained substantial (10–40%) throughout the 100–120 min in which new unbudded cells were being generated by cell division, and for ~20 min thereafter. Thus, the *CDC3* protein appeared to linger in a ring structure at the budding site for ≥20 min after cell division under these conditions. The results obtained with the *CDC12*-specific antibodies were similar, except that the proportions of unbudded cells displaying antigen rings were at all times smaller and more variable from experiment to experiment. Thus, the ring of *CDC12* polypeptide appeared to linger at the budding site for only a short time after cell division.

Examination of CDC3 and CDC12 Proteins in Shmoos and Zygotes

The association of the *CDC3* and *CDC12* proteins with the sites of cell wall reorganization and chitin deposition in budding cells suggested that these proteins might also be involved in the related processes that occur in cells that are mating or responding to mating pheromone (9, 26, 28, 36, 41, 42, 43; S. Ford and J. Pringle, manuscript in preparation). Indeed, after several hours of exposure to alpha factor, some shmoos (unbudded cells on which a broad protrusion has formed) exhibited faint but distinct bands of *CDC3* and *CDC12* immunofluorescence around the protruding regions (Fig. 5 *O*; and data not shown). This corresponded roughly with the regions of chitin deposition in these cells, as revealed by staining with Calcofluor (Fig. 5 *P*; reference 36). In mating cells, a faint band (or bands) of immunofluorescence in the region of fusion was often detectable soon after fusion with *CDC3*-specific antibodies (Fig. 5 *Q*, cells *a* and *b* and regions of cells *d* and *e* noted by *arrowheads*). Again, this localization corresponded roughly with the region of chitin deposition (Fig. 5 *R*). These immunofluorescence patterns were not detectable in all shmoos and zygotes, and it was not always clear that the structure stained was intracellular (see the problems with cell wall staining artifacts in reference 10). Thus, we cannot be certain that the association of the *CDC3* and *CDC12* proteins with the regions of cell wall reorganization is a normal feature of zygote and shmoo formation. It was clear, however, that as zygotes prepared to bud they formed rings of *CDC3* protein (Fig. 5 *Q*, cells *c* and *d*) and *CDC12* protein (not shown) that persisted as the buds emerged and enlarged (Fig. 5 *Q*, cells *e* and *f*), essentially as seen in budding vegetative cells.

Discussion

To study the intracellular organization and function of the yeast *CDC3* product, we raised antibodies against the fusion proteins encoded by in-frame fusions of *CDC3* to the *E. coli lacZ* and *trpE* genes. Antisera raised against each fusion protein were able to recognize both fusion proteins; this both demonstrated the presence of *CDC3*-specific antibodies and facilitated their effective affinity purification. Immunoblotting experiments using the purified antibodies revealed a single polypeptide of ~62 kD in extracts from normal yeast cells and a more abundant polypeptide of the same mobility in extracts from cells harboring a high-copy-number plasmid that contains the complete *CDC3* coding region (11, 25). The size of the presumed *CDC3* product agrees well with the 60 kD predicted from the sequence (11). In addition, the antibodies revealed an abundant polypeptide of ~50 kD in extracts from cells harboring a plasmid that appears to contain a *CDC3* gene that is truncated at its 5′ end (11). The size of this polypeptide is consistent with the hypothesis that its translation begins at the first available ATG (codon 70 of the normal *CDC3* coding region; reference 11). The retention of *cdc3*-complementing activity by this plasmid (25) suggests that the amino-terminal segment of the *CDC3* protein (a feature not shared with the other known members of this gene family; reference 11) is nonessential.

In view of the similarities in predicted amino acid sequence among the *CDC3*, *CDC10*, *CDC11*, and *CDC12* products (11), it is noteworthy that the *CDC3*-specific antibodies, like the *CDC12*-specific antibodies (10), showed no apparent cross-reaction with the other three gene products. Although it is possible that further testing may reveal weak cross-reactions, it seems likely that our immunofluorescence experiments have indeed revealed the localization of the *CDC3* product and not of a weakly cross-reacting species. As in previous studies (10, 23), affinity purification of the *CDC3*-specific antibodies was essential to avoid misleading immunofluorescence results due to other antibodies, present in all rabbit sera tested, that were reactive with yeast cell constituents.

The immunofluorescence localization of the *CDC3* product in wild-type cells revealed patterns similar to those observed with *CDC12*-specific (10) and *CDC10*-specific (H. B. Kim, S. Ketcham, and J. R. Pringle, manuscript in preparation) antibodies. These staining patterns suggest that all three gene products are associated with the ring of 10-nm filaments in the mother-bud neck. This hypothesis is supported by the immunofluorescence localization of the *CDC12* (10) and *CDC3* products in mutant strains. Localization of the *CDC3* product to the neck region was lost rapidly after a shift to restrictive temperature in *cdc10* or *cdc12* mutants, but not in *cdc11* or *cdc4* mutants, consistent with electron microscopic observations on the behavior of the 10-nm filaments in these strains (1; Byers, B., and L. Goetsch. 1976. *J. Cell Biol.* 70:35a; B. Byers and L. Goetsch, personal communication). Results with the *cdc3* mutant were more difficult to interpret; staining of the neck region with *CDC3*-specific antibodies was lost rapidly after the shift to restrictive temperature, although the electron microscopic observations suggest that the 10-nm filaments should remain in place until completion of the cell cycle in progress at the time of the temperature shift. Presumably, either the mutant *CDC3* product remains in the filaments but becomes unreactive to the antibodies after the temperature shift, or it dissociates from the filaments without destroying their higher-order structure.

The most economical interpretation of the available data is that the *CDC3*, *CDC10*, *CDC11*, and *CDC12* gene products are the primary constituents of the 10-nm filaments. As the

predicted amino acid sequences of these polypeptides show no extensive similarities to those of other known filament-forming proteins (11), the yeast 10-nm filaments would thus represent a novel type of eukaryotic cytoskeletal element. However, it also remains possible that the *CDC3*, *CDC10*, *CDC11*, and *CDC12* products are all accessory proteins that associate with a filamentous structure composed primarily of some as yet unidentified, but more conventional, filament-forming protein.

Electron microscopic observations have suggested that the 10-nm filaments assemble at the budding site coincident with early bud emergence and disassemble rather abruptly just before cytokinesis (4, 5). We attempted to explore further the assembly and disassembly processes using the *CDC3*-specific and *CDC12*-specific antibodies. Interpretation of our results is subject to three major caveats. First, as noted above, we do not know the degree to which either protein is responsible for the higher-order structure of the filaments as observed in the electron microscope. Thus, the presence of the *CDC3* and *CDC12* products at a given site may not necessarily imply the presence of filaments at that site, and vice versa. Second, the electron microscopic studies themselves suffer from the uncertainty that the filaments can be difficult to see even in budded cells, and would have been very difficult to see in unbudded cells (B. Byers, personal communication). Thus, it is possible that the filaments are actually assembled before bud emergence, or remain assembled at the budding site after cytokinesis, at least in some cells. Third, apparent differences in the behavior of the *CDC3* and *CDC12* polypeptides might reflect instead differences in the affinities of the respective antibodies.

With these caveats in mind, the following comments can be made. First, immunofluorescence observations using wild-type, nuclear division-mutant, and α-factor-arrested cells consistently indicated that the *CDC3* product remains localized to a ring structure at the old budding site on both mother and daughter cells after cytokinesis. The corresponding observations with respect to the *CDC12* product were less consistent (perhaps reflecting the variable efficacy of the immunofluorescence staining), but in aggregate suggest that this polypeptide may behave similarly. It appears that the *CDC3* and *CDC12* antigen rings then disappear gradually during the subsequent unbudded phase, at rates that may differ for *CDC3* and *CDC12*, and that may also vary from cell to cell. If we take the electron microscopic observations at face value, our results thus suggest that the higher-order structure of the filaments may disassemble before cytokinesis even though at least some of the filament-associated polypeptides remain localized to the region where the filaments had been. If there is a specific point in the cell cycle at which filament disassembly is triggered, it is apparently not reached in any of the mutants blocked in medial or late stages of nuclear division, as electron microscopic (Byers, B., and L. Goetsch. 1976. *J. Cell Biol.* 70:35a; B. Byers, personal communication) and immunofluorescence observations are consistent in indicating that filaments and filament-associated polypeptides remain in place at the mother-bud neck in arrested cells of these mutants. Cells blocked in nuclear division by the microtubule-disassembling drug nocodazole also retain 10-nm filaments at the mother-bud neck for extended periods, as judged by EM (19).

Second, immunofluorescence observations on exponentially growing and synchronized cultures consistently indicated that the *CDC3* product is localized to a ring structure at the presumptive budding site well before chitin-ring formation and the formation of buds visible by light microscopy ($\geq$15 min under the growth conditions used). The corresponding observations for *CDC12* were again less consistent, but in aggregate suggest that this polypeptide also may be localized to the budding site at least a few minutes before bud emergence. If we take the electron microscopic observations at face value (but note the caveat above), our results thus suggest that the higher-order structure of the filaments may assembly only some time after the known filament-associated polypeptides have been localized to the budding site.

In any case, the immunofluorescence observations appear to clarify the possible role of the 10-nm filaments in formation of the chitin ring. Such a role had been suggested by the evidence that the *cdc3*, *cdc10*, *cdc11*, and *cdc12* mutants, which lack the 10-nm filaments, also fail to form normal chitin rings, whereas other *cdc* mutants such as *cdc4*, which possess apparently normal 10-nm filaments, also form normal-looking chitin rings (Fig. 3, *C*, *E*, *G*, and *H*; Byers, B., and L. Goetsch. 1976. *J. Cell Biol.* 70:35a; references 1, 10; B. Byers, personal communication). This correlation might mean either that chitin-ring formation is dependent on the 10-nm filaments or the reverse, but support for the former interpretation was provided by the observations (*a*) that the *CDC3*, *CDC10*, and *CDC12* gene products all localize to the vicinity of the 10-nm filaments; and (*b*) that the *cdc10* and *cdc12* mutants lose preexisting filaments after a shift to restrictive temperature; taken together, these data suggest strongly that the primary lesions in these mutants involve formation of the 10-nm filaments. Moreover, a *chs1::URA3 csd2-1* mutant strain (3; C. Bulawa, personal communication), which produces little or no chitin, nonetheless shows apparently normal localization of the *CDC3*, *CDC10*, and *CDC12* products (our unpublished results), suggesting that filament formation is not dependent on the presence of a chitin ring. However the putative role for the 10-nm filaments in formation of the chitin ring was difficult to reconcile with the electron microscopic evidence that the filaments only form as the bud is emerging (5), whereas the chitin ring is well developed by that time (Fig. 4 *A*; references 16, 21). From our immunofluorescence studies, it now seems clear that at least some of the filament-associated polypeptides, if not actually the filaments themselves, are assembled at the budding site in time to play a role in chitin ring formation. However, it should also be noted that the 10-nm filaments and their associated polypeptides cannot be the only factors determining where chitin is deposited, as these elements appear equilaterally on both sides of the neck, whereas chitin is deposited only in the wall of the mother cell. A further consideration is the formation of septum-like structures at aberrant locations in *cdc3*, *cdc10*, *cdc11*, and *cdc12* mutants (38); one interpretation of these observations is that the 10-nm filaments are necessary for the normal positioning of the chitin ring, but not actually for its formation.

An approximate correlation between the distribution of the *CDC3* and *CDC12* products and the sites of cell wall reorganization and chitin deposition was also observed (with some significant uncertainties; see Results) in shmoos and zygotes. It is not clear whether the apparently diffuse localization of the *CDC3* and *CDC12* polypeptides in these cells

actually reflects the formation of 10-nm filaments in the corresponding regions, or whether these polypeptides can function without forming filaments.

The observation that the *CDC3* polypeptide, at least, appears at the presumptive budding site well in advance of bud emergence raises the very interesting questions of whether it is the 10-nm-filament-associated polypeptides or the actin network (2, 21, 30) that assembles first at the budding site, and of whether the later of these events is dependent upon the earlier. It should be noted that reorganizations of the actin network and of the 10-nm-filament-associated polypeptides are also temporally correlated at the end of the budding cycle (see above and refs. 2, 21, 30) and in shmoos and zygotes (see above; ref. 15; and S. Ford and J. Pringle, manuscript in preparation). We are currently investigating these issues.

We thank Breck Byers for his interest, helpful discussions, and the communication of unpublished results; Kevin Coleman for the original isolation of plasmid YEp13(CDC3)1; Sue Lillie for helpful discussions; and Susan Ford for providing the photomicrographs of Calcofluor-stained zygotes.

This work was supported by National Institutes of Health (NIH) grant GM31006 (to J. R. Pringle) and by predoctoral stipends to B. K. Haarer from The University of Michigan NIH Training Grants in Cellular and Molecular Biology (GM07315) and Developmental Biology (HD07274), The University of Michigan Center for Molecular Genetics, and The H. H. Rackham School of Graduate Studies.

Received for publication 27 August 1990 and in revised form 5 October 1990.

References

1. Adams, A. E. M. 1984. Ph.D. Thesis, The University of Michigan, Ann Arbor, Michigan.
2. Adams, A. E. M., and J. R. Pringle. 1984. Relationship of actin and tubulin distribution to bud growth in wild-type and morphogenetic-mutant *Saccharomyces cerevisiae*. *J. Cell Biol.* 98:934–945.
3. Bulawa, C. E., M. Slater, E. Cabib, J. Au-Young, A. Sburlati, W. L. Adair, Jr., and P. W. Robbins. 1986. The *S. cerevisiae* structural gene for chitin synthase is not required for chitin synthesis in vivo. *Cell.* 46:213–225.
4. Byers, B. 1981. Cytology of the yeast life cycle. *In* The Molecular Biology of the Yeast *Saccharomyces*: Life Cycle and Inheritance. J. N. Strathern, E. W. Jones, and J. R. Broach, editors. Cold Spring Harbor Laboratory, Cold Spring Harbor, NY. 59–96.
5. Byers, B., and L. Goetsch. 1976. A highly ordered ring of membrane-associated filaments in budding yeast. *J. Cell Biol.* 69:717–721.
6. Deleted in proof.
7. Cabib, E., R. Roberts, and B. Bowers. 1982. Synthesis of the yeast cell wall and its regulation. *Annu. Rev. Biochem.* 51:763–793.
8. Culotti, J., and L. H. Hartwell. 1971. Genetic control of the cell division cycle in yeast. III. Seven genes controlling nuclear division. *Exp. Cell Res.* 67:389–401.
9. Duntze, W., V. MacKay, and T. R. Manney. 1970. *Saccharomyces cerevisiae*: a diffusible sex factor. *Science (Wash. DC).* 168:1472–1473.
10. Haarer, B. K., and J. R. Pringle. 1987. Immunofluorescence localization of the *Saccharomyces cerevisiae CDC12* gene product to the vicinity of the 10-nm filaments in the mother-bud neck. *Mol. Cell. Biol.* 7:3678–3687.
11. Haarer, B. K., S. R. Ketcham, S. K. Ford, D. J. Ashcroft, and J. R. Pringle. 1990. The *Saccharomyces cerevisiae CDC3, CDC10, CDC11,* and *CDC12* genes encode a family of related proteins. *Genetics.* In press.
12. Hartwell, L. H. 1971. Genetic control of the cell division cycle in yeast. II. Genes controlling DNA replication and its initiation. *J. Mol. Biol.* 59:183–194.
13. Hartwell, L. H. 1971. Genetic control of the cell division cycle in yeast. IV. Genes controlling bud emergence and cytokinesis. *Exp. Cell Res.* 69:265–276.
14. Hartwell, L. H., R. K. Mortimer, J. Culotti, and M. Culotti. 1973. Genetic control of the cell division cycle in yeast. V. Genetic analysis of *cdc* mutants. *Genetics.* 74:267–286.
15. Hašek, J., I. Rupeš, J. Svobodová, and E. Streiblová. 1987. Tubulin and actin topology during zygote formation of *Saccharomyces cerevisiae*. *J. Gen. Microbiol.* 133:3355–3363.
16. Hayashibe, M., and S. Katohda. 1973. Initiation of budding and chitin-ring. *J. Gen. Appl. Microbiol.* 19:23–39.
17. Hinnen, A., J. B. Hicks, and G. R. Fink. 1978. Transformation of yeast. *Proc. Natl. Acad. Sci. USA.* 75:1929–1933.
18. Huffaker, T. C., J. H. Thomas, and D. Botstein. 1988. Diverse effects of beta-tubulin mutations on microtubule formation and function. *J. Cell Biol.* 106:1997–2010.
19. Jacobs, C. W., A. E. M. Adams, P. J. Szaniszlo, and J. R. Pringle. 1988. Functions of microtubules in the *Saccharomyces cerevisiae* cell cycle. *J. Cell Biol.* 107:1409–1426.
20. Kaback, D. B., P. W. Oeller, H. Y. Steensma, J. Hirschman, D. Ruezinsky, K. G. Coleman, and J. R. Pringle. 1984. Temperature-sensitive lethal mutations on yeast chromosome I appear to define only a small number of genes. *Genetics.* 108:67–90.
21. Kilmartin, J. V., and A. E. M. Adams. 1984. Structural rearrangements of tubulin and actin during the cell cycle of the yeast *Saccharomyces*. *J. Cell Biol.* 98:922–933.
22. Kilmartin, J. V., B. Wright, and C. Milstein. 1982. Rat monoclonal anti-tubulin antibodies derived by using a new nonsecreting rat cell line. *J. Cell Biol.* 93:576–582.
23. Lillie, S. H., and S. S. Brown. 1987. Artifactual immunofluorescent labeling in yeast, demonstrated by affinity purification of antibody. *Yeast.* 3:63–70.
24. Lillie, S. H., and J. R. Pringle. 1980. Reserve carbohydrate metabolism in *Saccharomyces cerevisiae*: responses to nutrient limitation. *J. Bacteriol.* 143:1384–1394.
25. Lillie, S. H., B. K. Haarer, L. Bloom, K. G. Coleman, and J. R. Pringle. 1990. Isolation and characterization of *CDC3, CDC11,* and *CDC12*, three genes controlling morphogenesis in the *Saccharomyces cerevisiae* cell cycle. *Genetics.* In press.
26. Lipke, P. N., A. Taylor, and C. E. Ballou. 1976. Morphogenic effects of α-factor on *Saccharomyces cerevisiae a* cells. *J. Bacteriol.* 127:610–618.
27. Maniatis, T., E. F. Fritsch, and J. Sambrook. 1982. Molecular Cloning: A Laboratory Manual. Cold Spring Harbor Laboratory, Cold Spring Harbor, NY 545 pp.
28. McCaffrey, G., F. J. Clay, K. Kelsay, and G. F. Sprague, Jr. 1987. Identification and regulation of a gene required for cell fusion during mating of the yeast *Saccharomyces cerevisiae*. *Mol. Cell. Biol.* 7:2680–2690.
29. Messing, J., B. Gronenborn, B. Müller-Hill, and P. H. Hofschneider. 1977. Filamentous coliphage M13 as a cloning vehicle: insertion of a *Hin*dII fragment of the *lac* regulatory region in M13 replicative form *in vitro*. *Proc. Natl. Acad. Sci. USA.* 74:3642–3646.
30. Novick, P., and D. Botstein. 1985. Phenotypic analysis of temperature-sensitive yeast actin mutants. *Cell.* 40:405–416.
31. Paquin, C., and J. Adams. 1982. Isolation of sets of *a*, α, *a*/α, *a*/*a* and α/α isogenic strains in *Saccharomyces cerevisiae*. *Curr. Genet.* 6:21–24.
32. Pringle, J. R., and J.-R. Mor. 1975. Methods for monitoring the growth of yeast cultures and for dealing with the clumping problem. *Methods Cell Biol.* 11:131–168.
33. Pringle, J. R., and L. H. Hartwell. 1981. The *Saccharomyces cerevisiae* cell cycle. *In* The Molecular Biology of the Yeast *Saccharomyces*: Life Cycle and Inheritance. J. N. Strathern, E. W. Jones, and J. R. Broach, editors. Cold Spring Harbor Laboratory, Cold Spring Harbor, NY. 97–142.
34. Pringle, J. R., S. H. Lillie, A. E. M. Adams, C. W. Jacobs, B. K. Haarer, K. G. Coleman, J. S. Robinson, L. Bloom, and R. A. Preston. 1986. Cellular morphogenesis in the yeast cell cycle. *In* Yeast Cell Biology (UCLA Symposia on Molecular and Cellular Biology. Vol. 33). J. Hicks, editor. Alan R. Liss, New York. 47–80.
35. Rüther, U., and B. Müller-Hill. 1983. Easy identification of cDNA clones. *EMBO (Eur. Mol. Biol. Organ.) J.* 2:1791–1794.
36. Schekman, R., and V. Brawley. 1979. Localized deposition of chitin on the yeast cell surface in response to mating pheromone. *Proc. Natl. Acad. Sci. USA.* 76:645–649.
37. Sherman, F., G. R. Fink, and J. B. Hicks. 1986. Methods in Yeast Genetics. Cold Spring Harbor Laboratory, Cold Spring Harbor, NY. 186 pp.
38. Slater, M. L., B. Bowers, and E. Cabib. 1985. Formation of septum-like structures at locations remote from the budding sites in cytokinesis-defective mutants of *Saccharomyces cerevisiae*. *J. Bacteriol.* 162:763–767.
39. Sloat, B. F., and J. R. Pringle. 1978. A mutant of yeast defective in cellular morphogenesis. *Science (Wash. DC).* 200:1171–1173.
40. Sloat, B. F., A. Adams, and J. R. Pringle. 1981. Roles of the *CDC24* gene product in cellular morphogenesis during the *Saccharomyces cerevisiae* cell cycle. *J. Cell Biol.* 89:395–405.
41. Thorner, J. 1981. Pheromonal regulation of development in *Saccharomyces cerevisiae*. *In* The Molecular Biology of the Yeast *Saccharomyces*: Life Cycle and Inheritance. J. N. Strathern, E. W. Jones, and J. R. Broach, editors. Cold Spring Harbor Laboratory, Cold Spring Harbor, NY. 143–180.
42. Tkacz, J. S., and V. L. MacKay. 1979. Sexual conjugation in yeast: cell surface changes in response to the action of mating hormones. *J. Cell Biol.* 80:326–333.
43. Trueheart, J., J. D. Boeke, and G. R. Fink. 1987. Two genes required for cell fusion during yeast conjugation: evidence for a pheromone-induced surface protein. *Mol. Cell. Biol.* 7:2316–2328.
44. Wilkinson, L. E., and J. R. Pringle. 1974. Transient G1 arrest of *S. cerevisiae* cells of mating type α by a factor produced by cells of mating type *a*. *Exp. Cell Res.* 89:175–187.